



ELSEVIER

FEMS Microbiology Letters 248 (2005) 83–91

FEMS
 MICROBIOLOGY
 Letters

www.fems-microbiology.org

The expression of selected non-ribosomal peptide synthetases in *Aspergillus fumigatus* is controlled by the availability of free iron

Kathrin Reiber^a, Emer P. Reeves^a, Claire M. Neville^a, Robert Winkler^{a,b},
 Peter Gebhardt^{a,b}, Kevin Kavanagh^a, Sean Doyle^{a,*}

^a National Institute for Cellular Biotechnology, Department of Biology, National University of Ireland, Maynooth, Co. Kildare, Ireland

^b Hans-Knoell-Institute for Natural Product Research, Department of Biostructure Chemistry, Jena, Beutenbergstr. 11, D-07745, Germany

Received 7 April 2005; received in revised form 12 May 2005; accepted 16 May 2005

First published online 31 May 2005

Edited by G.M. Gadd

Abstract

Three non-ribosomal peptide synthetase genes, termed *sidD*, *sidC* and *sidE*, have been identified in *Aspergillus fumigatus*. Gene expression analysis by RT-PCR confirms that expression of both *sidD* and *C* was reduced by up to 90% under iron-replete conditions indicative of a likely role in siderophore biosynthesis. *SidE* expression was less sensitive to iron levels. In addition, two proteins purified from mycelia grown under iron-limiting conditions corresponded to SidD (~200 kDa) and SidC (496 kDa) as determined by MALDI ToF peptide mass fingerprinting and MALDI LIFT-ToF/ToF. Siderophore synthetases are unique in bacteria and fungi and represent an attractive target for antimicrobial chemotherapy.

© 2005 Federation of European Microbiological Societies. Published by Elsevier B.V. All rights reserved.

Keywords: NRPS; Iron; Siderophore; MALDI ToF; Secondary metabolites; Proteomics; 4'-PPTase

1. Introduction

The fungus *Aspergillus fumigatus* is receiving increasing attention as a significant cause of mortality in immunocompromised individuals such as bone marrow and stem cell transplant patients [1]. The near-completion of the *A. fumigatus* genome sequencing effort and resultant data [2] has greatly facilitated the search for genes which may be involved in mediating organismal pathogenicity and a number of reports have shown that either specific gene deletion or silencing may downregulate the virulence of *A. fumigatus* [3–5]. Hissen et al. [6] have convincingly argued that siderophores produced by the fungus are involved in iron acquisition from transferrin

and that, at least in vitro, they may be responsible for organism growth and survival in human serum.

Most members of the family Ascomycota (e.g., *A. fumigatus*) produce hydroxamate-type siderophores. Hydroxamates can be sub-divided into four groups: rhodotorulic acid, fusarinines, coprogens and ferrichromes. *A. fumigatus* produces ferrichrome class siderophores (e.g., ferricrocin), which are cyclic peptides [7]. In addition, a number of siderophores (primarily triacetylfusarinine C and ferricrocin) were purified from *A. fumigatus* culture medium after 8 h of growth in medium containing human serum [6].

In *Aspergillus nidulans*, siderophore biosynthesis commences with the N⁵-hydroxylation of ornithine, followed by transacylation and subsequent covalent assembly of the modified ornithine residues with or without further amino acids (e.g., serine, alanine and glycine),

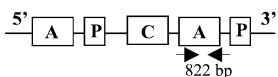
* Corresponding author. Tel.: +353 1 7083858; fax: +353 1 7083845
 E-mail address: sean.doyle@nuim.ie (S. Doyle).

catalyzed by non-ribosomal peptide synthetases (NRPS) [8,9]. NRPS are multifunctional enzymes, which operate via a thiotemplate mechanism [10] and consist of semi-autonomous units or modules (Fig. 1), co-linearly arranged to the structure of the peptide product. A typical module minimally consists of an adenylation domain (A-domain), responsible for the activation of its cognate substrate amino acid as an amino acyl adenylate, a downstream located peptidyl carrier protein (PCP or P) or thiolation domain and an upstream positioned condensation domain (C-domain) [11]. Siderophores are predominantly released by cyclization of the peptide product, often catalyzed by cyclotrimerizing TE-domains (e.g., enterobactin, yersiniabactin) or variants of the condensation domains, termed as cyclization domains [12,13]. Furthermore, the iterative (repetitive) use of the enzyme template, as well as a non-linear structure (e.g., –P–C–P–C–), seems to be characteristic of siderophore synthetases. *SidC*, an NRP synthetase involved in ferricrocin biosynthesis in *A. nidulans*, encodes a 525.5 kDa protein comprising three adenylation, five condensation and five thiolation domains [9,14]. In spite of only three complete modules, the entire hexapeptides of the cyclic hydroxamate-type siderophores, such as

triacetylfusarinine C and ferricrocin are formed by repeated use of modules. Furthermore, *sidA* encodes an L-ornithine-N⁵-monooxygenase which catalyzes the first step in the siderophore biosynthesis pathway in *A. nidulans* [9]. Deletion of the *sidA* gene completely inhibited siderophore biosynthesis in *A. nidulans* and resulted in severely diminished fungal viability. The *sidA* ortholog in *A. fumigatus* has been recently reported and deletion mutants show a distinct reduction in virulence [3]. *Ustilago maydis*, an infectious agent of maize, scavenges iron using extracellular hydroxamate siderophores, where siderophore production is initiated by the *sidI* gene. However, analysis of siderophore mutants in *U. maydis* suggests that the siderophore biosynthetic pathway is not involved in the infection of maize [15]. More recently, Yuan et al. [16] have identified an NRP synthetase gene (*sid2*) involved in ferrichrome biosynthesis in *U. maydis*. Expression of *sid2* was upregulated (×2.5) in low-iron compared to high-iron media.

We have detected a number of putative NRPS open reading frames in the genome of *A. fumigatus* and recently demonstrated in vitro NRPS (termed Pes1/SidB) activation by a functional 4'-phosphopantetheinyl transferase [17]. Evidence is now presented that at least three distinct NRPS genes are susceptible to regulation of expression by the level of free iron present in the culture medium.

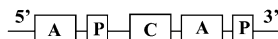
SidD (*A. fumigatus*): 5745 bp (1915 aa)



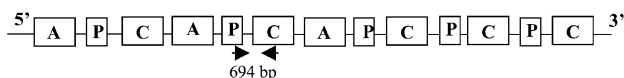
% identity: 75

Sid2 (*A. oryzae*): 5775 bp (1924 aa)

% similarity: 85



SidC (*A. fumigatus*): 13 551 bp (4517 aa)



% identity: 55

SidC (*A. nidulans*): 19 160 bp (4793 aa)

% similarity: 71



SidE (*A. fumigatus*): 6330 bp (2109 aa)

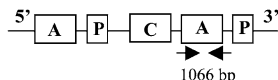


Fig. 1. Modular organization of three non-ribosomal peptide synthetase genes from *Aspergillus fumigatus*: *sidD*, *C* and *E*, and relevant orthologs (i.e., *sid2* of *A. oryzae* and *sidC* of *A. nidulans*). Where available, the degree of identity and similarity is indicated. Single catalytic units of NRPS are indicated as follows: A, adenylation; P, thiolation and C, condensation domain. The position of PCR amplified and sequenced regions is marked by arrows and has been deposited in GenBank. Preliminary data were obtained from <http://www.tigr.org>.

2. Materials and methods

2.1. Microorganisms and culture media

Aspergillus fumigatus ATCC 26933 (obtained from the American Type Culture Collection, Manassas, VA, USA) was used in this study and maintained as spore suspensions containing 50% (v/v) glycerol at –80 °C. The fungus was grown in a mineral salt medium (pH 6.8) composed of 25 g/l glucose, 3.5 g/l (NH₄)₂SO₄, 2.0 g/l KH₂PO₄, 0.5 g/l MgSO₄ and 8 mg/l ZnSO₄ and supplemented with different concentrations of Fe(III)Cl₃, as required. *A. fumigatus* cultures were set up in 500 ml shaking flasks at 230 rpm, previously treated to ensure that all traces of iron were removed from the glassware [6]. Medium (250 ml) was inoculated with *A. fumigatus* conidia at a final concentration of 10⁷ per ml and flasks were incubated at 37 °C and 230 rpm.

2.2. Bioinformatic analyzes

Preliminary *A. fumigatus* sequence data were obtained from The Institute for Genomic Research website at <http://www.tigr.org>. The unannotated *A. fumigatus* genome was interrogated, via a BLAST program, for non-ribosomal peptide synthetase encoding open reading frames (ORFs) using the *Acremonium chrysogenum*

alpha-aminoadipyl-cysteinyl-D-valine-synthetase (ACVS) encoding gene (GenBank Accession No. E05192) and *Aspergillus nidulans* peptide synthetase (*sidC*) gene (GenBank Accession No. AY223812). Putative NRPS-encoding ORFs, from the *A. fumigatus* genome, were aligned to other peptide synthetases using Clustal W (<http://www.ebi.ac.uk/clustalw/>). Bootstrap neighbor joining phylogenetic trees, using the resulting alignment, were drawn using the tree finder program (<http://taxonomy.zoology.gla.ac.uk/rod/treeview.html>).

2.3. Detection and quantification of siderophores

Siderophore production in *A. fumigatus* was investigated using the Chrome Azurol S (CAS) assay [18,19].

2.4. DNA/RNA isolation and RT-PCR

Filtered and washed *A. fumigatus* hyphae, collected at appropriate culture time-points, were crushed using a mortar and pestle under liquid nitrogen. All DNA and RNA manipulations were carried out as recently described [20]. To facilitate equal amounts of RNA for cDNA synthesis and RT-PCR, densitometric measurements of rRNA on RNA agarose gels were performed. PCR of genomic or cDNA was performed using AccuTaq polymerase (Sigma–Aldrich), 1–10 ng genomic DNA and 0.5 μ M each of forward and reverse primer in a total volume of 20 μ l. PCR conditions were as follows: 96 °C denaturation for 3 min; (93 °C denaturation for 30 s, 65 °C annealing for 90 s, 68 °C extension for 90 s) \times 45 cycles; 68 °C extension for 7 min. PCR was performed using primers *sidD*-forward (5'-ACGCAACCGACTGGTTGTT-3'), *sidD*-reverse (5'-ATTCGTGCGAGACTCGGAT-3'); *sidC*-forward (5'-CCGATTATGCACATCCTCTTCC-3'), *sidC*-reverse (5'-CCAGAATCTTCGGGTCTC-3'), *sidE*-forward (5'-GAGCCAGCTGACGAGATTGAT-3') *sidE*-reverse (5'-GGAGCGCTTGTTAAACAACCT-3'). The gene encoding calmodulin, which is constitutively expressed in *A. fumigatus*, served as a control in RT-PCR experiments and was amplified across an intron–exon boundary [21]. Optimal cDNA amplification was found to require 45 cycles of PCR. PCR-amplified DNA was electrophoresed, visualized and subjected to semi-quantitative expression analysis as recently described [20].

2.5. Protein purification

All protein purification steps were performed at 4 °C. Mycelia were harvested by filtration and washed twice in phosphate-buffered saline (PBS, pH 7.4). Washed mycelia were resuspended in Buffer A (100 mM Tris, 50 mM NaCl, 20 mM EDTA, 30 mM DTT, 44.71 mg/l PMSF, 2 mg/l DNaseI, 300 mg/l lysozyme, 21 mg/l leupeptin,

10 mg/l TLCK, 10 mg/l pepstatin A and 10% (v/v) glycerol, pH 7.3 [22]) and passed through a French press (700–1000 bar). Cell debris was removed by centrifugation at 40,000g for 30 min. Supernatant was concentrated by Q-Sepharose™ anion-exchange chromatography (load/wash: Buffer A without NaCl; elution: Buffer A + 1 M NaCl; bed volume: 20 ml; protein load: 80 mg). Selected fractions, identified by SDS–PAGE (data not shown), containing high molecular mass proteins were further purified by gel permeation chromatography over a Superose 6 resin (10 \times 300 mm; flow rate 1.0 ml/min; 100 mM Tris, 50 mM NaCl, 20 mM EDTA, 30 mM DTT and 10% (v/v) glycerol, pH 7.3.) using an ÄKTA purifier 100 system (Amersham Bioscience, Sweden). Protein concentrations were determined using the Bradford assay [23] with BSA as standard. SDS–PAGE was performed according to the method of Laemmli [24] using high molecular mass protein calibration (Sigma–Aldrich).

2.6. Two-dimensional electrophoresis

After gel permeation chromatography, selected protein-containing fractions were also subject to separation by 2D-PAGE. Protein (200 μ g) was precipitated with 5 volumes of ice-cold 100% acetone and air-dried. Pellets were resuspended in 250 μ l IEF-buffer (10 mM Tris, 8 M urea, 2 M thiourea, 4% (w/v) CHAPS, 1% (v/v) Triton X-100, 65 mM DTT and 0.8% (w/v) ampholyte), loaded onto linear immobilized pH gradient (IPG) strips (13 cm, pH range: 3–10) and isoelectric focussing (IEF) was performed at 16 °C using an Ettan™ IPGphorII™ instrument (Amersham Bioscience). After a conditioning step at 50 V for 10 h, 250 V was held over 15 min, followed by voltage ramping to 8000 V in 5 h, which was held for further 8 h. IPG strips were then incubated twice in 15 ml equilibration buffer (50 mM Tris, 30% (v/v) glycerol, 2% (w/v) SDS and 6 M urea, pH 6.8), supplemented with 2% (w/v) DTT and subsequently with 2.5% (w/v) iodoacetamide for 20 min. The strips were then placed on a 7.5–10% (w/w) SDS–PAGE gel and electrophoresed overnight at 80 V at 4 °C.

2.7. Mass spectrometry

Protein samples for peptide mass determination were separated by SDS–PAGE or 2D-PAGE, excised from the gels and digested with trypsin (Promega sequencing grade; 5–20 μ g, overnight). The resultant peptide mixtures were extracted from gel pieces, mixed with saturated α -cyano-4-hydroxycinnamic acid as previously described [17] and mixtures (0.5 μ l) applied to MTP 384 ground steel mass spectrometry targets (Bruker) and allowed to dry. Matrix Assisted Laser Desorption/Ionization-Time of Flight Mass Spectrometry (MALDI ToF MS) was performed using a Bruker ultraflex

LIFT-ToF/ToF (UK). Determination of tryptic fingerprints was carried out on different spots of one sample, and device parameters, especially laser power, adjusted until an optimal signal/noise ratio was found. Mass spectra with high signal intensity were subjected to LIFT-ToF/ToF analysis [25]. Spectra were processed using FlexAnalysis software (Bruker), using tryptic fragments of trypsin for internal calibration of spectra. Database searches and sequence comparisons were carried out via Mascot in-house server (MatrixScience) and Biotoools (Bruker), respectively.

3. Results and discussion

3.1. Molecular characterization and phylogenetic analysis of three NRPS-encoding genes *sidD*, *C* and *E*

After interrogation of the *A. fumigatus* genome by BLAST analysis, using the ACVS- and *A. nidulans* peptide synthetase (*sidC*) encoding genes, several ORFs, encoding NRPS were identified. *AfusidD* and *C* (GenBank Accession Nos. DQ013888 and DQ011870) clustered with known and proposed siderophore synthetases upon phylogenetic analysis (data not shown). According to the modular organization (Fig. 1) and strong resemblance, *sidD* (GenBank Accession No. DQ011871) is likely to be an ortholog of *sid2*, a putative siderophore synthetase encoding gene of *Aspergillus oryzae* (GenBank Accession No. AB087617). Both sequences showed 75% identity (85% similarity). Like *sid2*, *sidD* encodes a bi-modular NRPS consisting of two adenylation, two thiolation and one condensation domain. SidD comprises 1915 amino acids corresponding to an estimated molecular mass of 210 kDa. The eight-amino acid motif within adenylation domains, which has a predominant influence on the formation of the substrate-specific pocket [26,27], was determined

for module 1 of the putative SidD and Sid2 (Table 1). Both motifs are identical (DVGGGGI), thereby predicting that 5-hydroxy-ornithine is recognized and activated by the first adenylation domain ([28]; <http://raynam.chm.jhu.edu/~nrps/instructions.html>). 5-Hydroxy-ornithine is the main constituent of hydroxamate siderophores. The A-domain in module 2 of *sidD* and *sid2* (Table 1) seemed to be degenerate and only 51 amino acids (instead of around 450) show sequence similarity to other adenylation domains. Hence, no prediction with respect to amino acid motif was possible and it is proposed that only the first module is capable of amino acid incorporation. The presence of a thiolation domain on the last position of a NRPS is unusual. It may serve as a “linker” domain to facilitate repetitive use of SidD-domains or interaction with another NRPS, to which the partially formed peptide is transferred for further modification [29]. A similar working principle with two interacting NRP synthetases was suggested for peptaibol formation in *Sepedonium ampullosporum* [30]. In addition, a multi-subunit NRP synthetase complex is present in *C. purpurea*, which directs ergot peptide formation and was the first identified fungal NRP synthesis system containing different subunits [31].

The ORF encoding *sidC* in *A. fumigatus* appeared to be an ortholog of *sidC*, which encodes an NRPS involved in hydroxamate siderophore (ferricrocin) biosynthesis in *A. nidulans* [8]. Both describe a similar modular structure (Fig. 1) with sequence identity of 55% (similarity: 71%). The 13,551 bp ORF of *AfusidC* predicted a protein of 4517 amino acids (molecular mass: 496 kDa). AfuSidC clusters together with both AniSidC and Sid2, a ferrichrome siderophore peptide synthetase gene by *U. maydis* (GenBank Accession No. U62738), indicating a functional relationship. Similar amino acid codes were found for the corresponding adenylation modules (Table 1) in AniSidC and AfuSidC. Thus, almost the same amino acids were predicted to be

Table 1
Prediction of the theoretical substrate amino acids activated by the single adenylation domains of SidD, C and E from *A. fumigatus*

Predicted amino acid incorporation	Module (m)	Signature motif							
		1	2	3	4	5	6	7	8
5(OH)Orn	AfuSidD-m1	D	V	D	G	G	G	G	I
5(OH)Orn	AorSid2-m1	D	V	D	G	G	G	G	I
–	AfuSidD-m2	Not predictable							
–	AorSid2-m2	Not predictable							
Ala	AfuSidC-m1	D	P	M	M	W	M	A	I
Ala	AniSidC-m1	D	P	M	M	W	M	A	I
–	AfuSidC-m2	D	V	Q	H	T	I	T	I
–	AniSidC-m2	D	V	Q	H	T	I	T	V
Gly/Ser	AfuSidC-m3	D	V	L	S	S	G	A	I
Tyr/Trp/Gly	AniSidC-m3	D	P	L	S	T	G	A	I
–	AfuSidE-m1	Not predictable							
Val	AfuSidE-m2	D	V	Y	F	T	G	G	V

Comparison with putative ortholog sequences Sid2 (*A. oryzae*) and SidC (*A. nidulans*) according to the NRPS prediction blast server ([28]; <http://raynam.chm.jhu.edu/~nrps/instructions.html>).

recognized and activated by the adenylation domains of module one (alanine) and three (glycine or serine) of both genes according to NRPS adenylation domain prediction [28]. Alanine, glycine and serine might be charged by the domains of AfuSidC, which are thereby constituents of the hydroxamate siderophore ferricrocin, produced by *A. fumigatus* [32].

SidE comprises a 6330 bp ORF and encoded a theoretical bi-modular NRPS-protein of 2109 amino acids. Like AfuSidD, this hypothetical protein (SidE) appeared to contain two adenylation and thiolation domains and one condensation domain (Fig. 1). SidE shared 24% amino acid identity (42% similarity) with AfuSidC and both proteins may be derived from a common ancestor. In addition, SidE clustered with *A. nidulans* SidC and Sid2 of *U. maydis* following phylogenetic analysis whereby 25% identity/42% similarity and 23% identity/40% similarity, respectively, is evident. While no prediction was possible for the substrate amino acid encoded by module 1 of SidE, module 2 contains the eight-amino acid non-linear motif, DVYFTGGV, and predicted incorporation of valine (Table 1) [28].

3.2. Siderophore production

Fig. 2 shows that optimal siderophore production occurred when *A. fumigatus* was grown in the absence of iron. Furthermore, significantly higher siderophore amounts were apparent at the 72 h time-point following culture under iron-free conditions compared to earlier time-points ($p < 0.05$). Significant diminution of siderophore levels was apparent ($p < 0.05$) under 20 μM iron conditions (up to 2-fold), although total levels present at 72 h time-point were approximately 50% of those evident under iron-free conditions. Low siderophore production was evident, and minimal differences in siderophore levels were detectable, at any time-point, under high iron (300 μM) culture conditions. Moreover, maximum siderophore productions under high iron conditions were between 2- and 15-fold less than those observed under iron free or low iron culture conditions.

It has recently been demonstrated that *sidA* expression in *A. fumigatus* is upregulated under conditions of iron starvation (12–24 h culture time) [3]. Moreover, dramatic increases in the levels of extracellular TAFC and intracellular desferriferricrocin were concomitantly observed [3]. Hissen et al. [6] have demonstrated that siderophore production by *A. fumigatus* is significantly greater in the presence of holo-transferrin, as opposed to serum, in minimal essential medium (MEM) over a 19-h incubation time and that Fe(III) (20 μM) already causes iron limitation which results in induction of enhanced siderophore formation and excretion. In the present study, where minimal media containing glucose and several salts were supplemented with different concentrations of Fe(III), this finding was confirmed. These

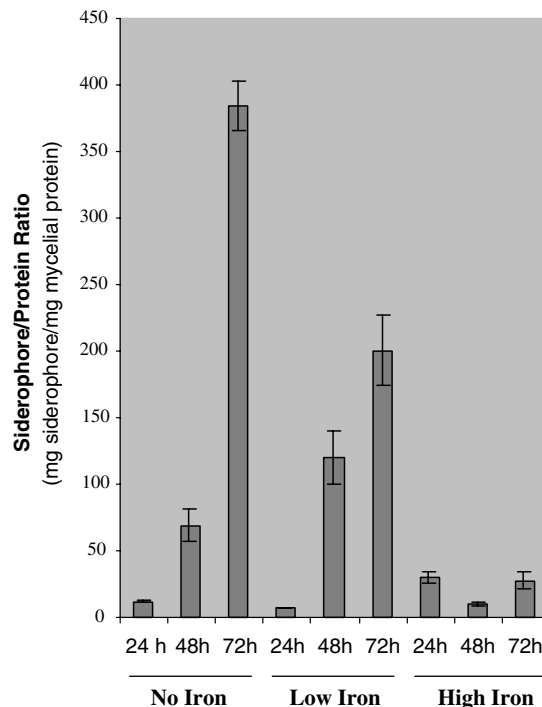


Fig. 2. Quantitation of siderophore production by *A. fumigatus* under differential iron concentrations (0, 20 and 300 μM). Maximum siderophore production was induced when *A. fumigatus* was grown in the absence of iron. Diminution of siderophore production is apparent under low iron conditions (20 μM). Low siderophore levels were evident when the fungus was grown in the presence of 300 μM Fe(III).

data clearly demonstrate that siderophore production is enhanced in the absence of free iron.

3.3. Expression analysis of *sidD*, *C* and *E*

Expression of *sidD*, *C* and *E* was assessed by semi-quantitative RT-PCR analysis. rRNA loading was used as a control to ensure equal amounts of RNA used for cDNA synthesis (Fig. 3A). The presence of genomic DNA was excluded by both DNase treatment of isolated RNA prior to RT-PCR and analysis of the size difference between the genomic and cDNA amplicon of *calm* from which introns have been excised (Fig. 3B). It can be seen that *sidD* and *C* expression was evident at all time points during *A. fumigatus* growth from $T = 24$ –72 h in the absence of free iron and that diminution of expression occurs both under low (20 μM) and high (300 μM) iron conditions (Fig. 3C and D). Expression of *sidD* diminished by between 25% and 60% under low iron conditions and by up to 90% under high iron conditions (24 and 48 h), upon comparison to *sidD* expression in the absence of free iron. Although *sidD* exhibits 75% sequence identity with *sid2* of *A. oryzae*, no information is available on the expression pattern of *sid2* and so a comparative analysis was not possible.

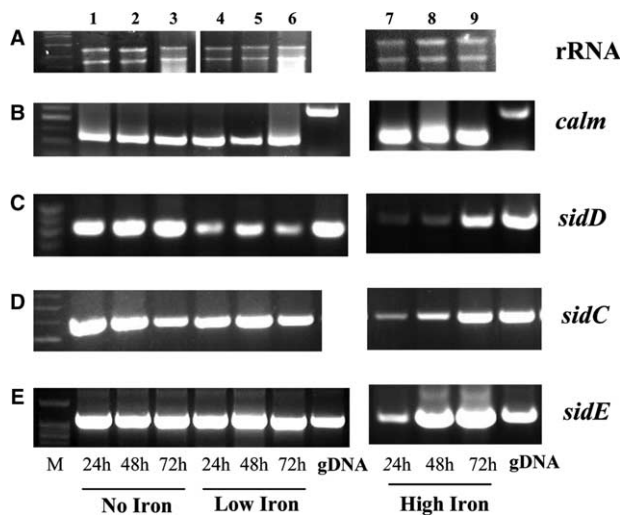


Fig. 3. RT-PCR analysis of the regulative response of non-ribosomal peptide synthetase genes in *A. fumigatus* (*sidD*, *C* and *E*) in the presence and absence of free iron. Lanes 1–9 contain RNA or cDNA amplicons obtained after 24, 48 and 72 h of cultivation in no iron supplemented WB-medium (1–3), low iron supplemented WB-medium (20 μ M, 4–6) and high iron concentrations in WB-medium (300 μ M, 7–9). PCR on genomic DNA (gDNA) served as a control in RT-PCR experiments. (A) Equivalent amounts of RNA were used for all cDNA synthesis and amplification reactions as judged by rRNA. (B) RT-PCR analysis of the house-keeping gene (calmodulin) confirmed the absence of DNA (intron excision) and further confirmed mRNA/cDNA integrity. (C) The putative siderophore synthetase encoding gene, *sidD*, demonstrates a diminution of expression with increasing iron availability, as judged by RT-PCR analysis. (D) *SidC* shows a weaker, but similar, regulation response. (E) Expression of *sidE* appears to be unaffected by available Fe(III), unlike that of *sidD* or *sidC*, under all investigated culture conditions except at the 24 h time-point under high iron conditions.

Expression of *sidC* appeared to be maintained under low iron conditions compared to that of *sidD*, but was reduced by approximately 65–80% under high iron conditions (24 and 48 h) relative to expression in iron-free culture conditions. Yuan et al. [16] have observed a similar phenomenon when *U. maydis* was cultured in low iron medium whereby a 2.5-fold increase in *sid2* expression was determined by Northern hybridization. Interestingly, expression of both *sidD* and *C* appeared to be upregulated under high iron conditions at the 72 h time-point, possibly due to depletion of iron in the medium as fungal growth proceeds. Constitutive and constant expression of *sidE* was observed under all experimental conditions, except during the early growth phase under high iron conditions (24 h) where a 65% decrease in expression is evident relative to culture in the absence of iron at 24 h. Although previous work has also shown that the expression of *A. nidulans sidC* is negatively regulated by the presence of iron (10 μ M) [33], the results presented here are the first demonstration that the expression of up to three NRPS-encoding genes in *A. fumigatus* is differentially regulated by iron availability.

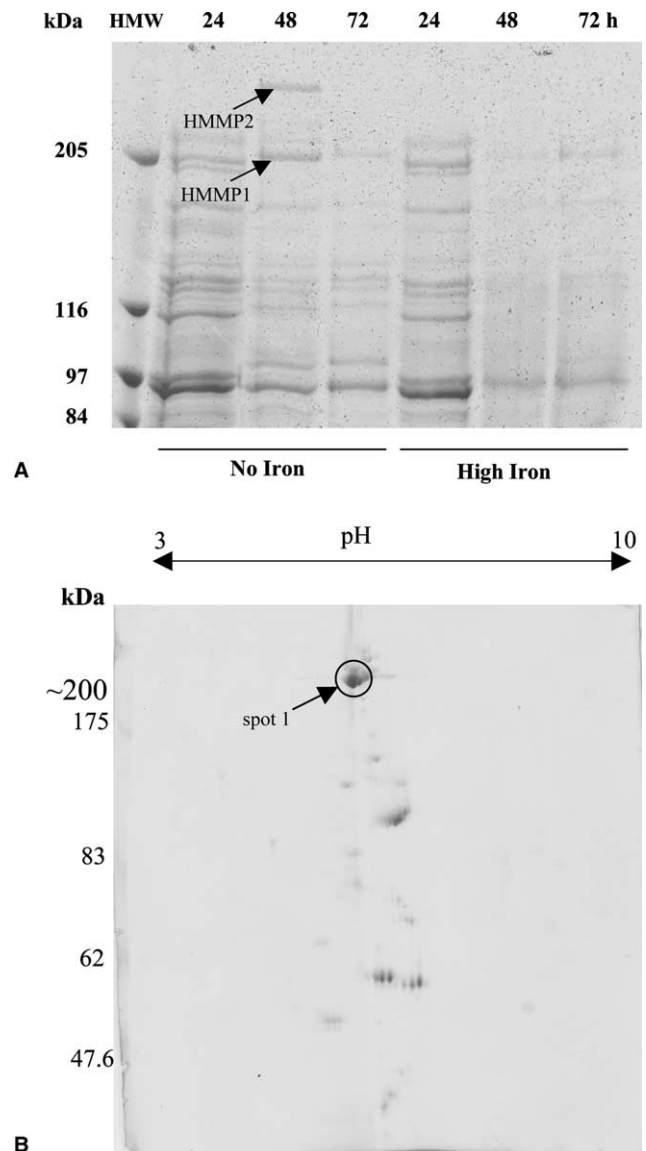


Fig. 4. (A) SDS-PAGE analysis of high molecular mass (HMM) proteins extracted from *A. fumigatus* cultures grown under strong iron limitation (no additional iron supply) and sufficient (300 μ M) iron supply. Equivalent protein amounts (376 μ g) were loaded to examine differential protein expression over a time course of 3 days (24, 48 and 72 h). Two high molecular mass proteins, termed HMMP1 and 2, were upregulated under conditions of iron limitation, especially at the 48 h time-point and were subsequently analyzed by MALDI-ToF mass spectrometry. (B) 2D-PAGE further resolved a number of proteins (at least three) which appear at a molecular size of approx. 200 kDa. The spot (circled) was analyzed by MALDI-ToF mass spectrometry. (C) The MALDI LIFT-ToF/ToF mass spectrum of a peptide of 1498.744 Da, corresponding to a *SidD* fragment. The amino acid (aa) sequence, analyzed by PSD (post-source decay) fragmentation, confirms N- (2 aa) and C-terminal (4 aa) sequence: C-terminal (y-fragments): RARL; N-terminal (b-fragments): VE, confirming a peptide sequence: VEXXXXXXXLRAR. Internal fragments cover the remainder of the peptides: LG (y11b4) and GEIESQLRA (y10b12). Thus, the following amino acid sequence VELGEIESQLRAR of HMMP1 matches 100% to the theoretical one of *SidD* and confirms HMMP1 as the *sidD*-encoded NRPS. Inset: peptide mass fingerprint of trypsin-digested *SidD*. (D) Peptide mass fingerprint of trypsin-digested HMMP2.

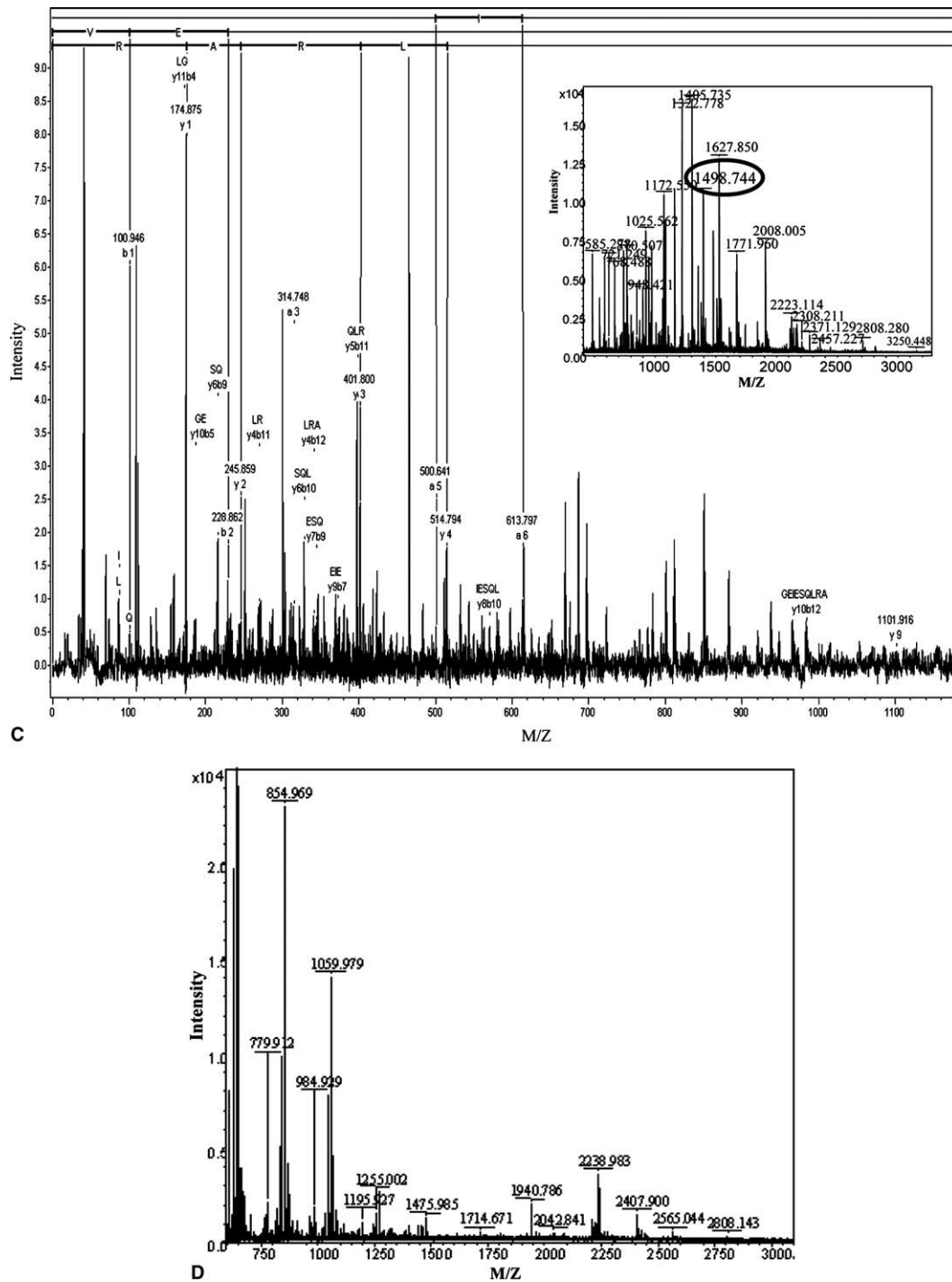


Fig. 4. (continued)

3.4. Protein expression analysis

Protein extracts of *A. fumigatus* cultures grown with and without free iron over a time course of 3 days were prepared and subjected to SDS-PAGE analysis. Two proteins, one of approximate molecular mass 200 kDa, termed high molecular mass protein (HMMP)1, and another of 300–400 kDa, termed HMMP2, were predomi-

nantly expressed at 48 h, in the absence of iron (Fig. 4A). Expression of HMMP1 was still evident at 72 h, moreover, this protein also seems to appear at a later time-point (72 h) in the high-iron containing medium. The protein expression profile of HMMP1 indicated resemblance to the transcript course of *sidD*, which encodes a 210 kDa NRP synthetase (Fig. 3). HMMP1 (approx. 200 kDa) was partially purified by means of

Table 2

Tryptic peptides of HMMP1 and post-source decay (PSD) fragmentation, analyzed by MALDI LIFT-ToF/ToF, using the “LIFT” technique in comparison to the amino acid sequence of corresponding tryptic peptides of the theoretical SidD-protein

Parent mass/SidD-MH + (monoisotopic)	Actual sequence from LIFT spectrum	Theoretical SidD amino acid sequence (domain of origin)
1186.608/1187.621	LQNXQXVXXK	LQNMAQQVGAK (A1)
1322.773/1323.654	YXIXEDSADXXR	YAIVEDSADGKR (C1)
1424.750/1424.758	AQMRDFXRXR	AQMRDFVRFVR (C1)
2344.243/2344.136	TXAAXIXXPWLXXXHXXXPXX	TAAAFIEDPSWLVAGHEGYPR (A1)

Highlighted amino acids are identical in both actual and predicted SidD-derived peptides. Peptides originate from either adenylation (A) or condensation (C) domain 1 of SidD.

ion-exchange and gel permeation chromatography (Fig. 4B). Pooled gel permeation column fractions, containing HMMP1, were further separated by 2D-PAGE. As can be seen in Fig. 4B, up to three proteins of equivalent molecular mass (approx. 200 kDa) were present. Peptide mass fingerprinting of the most abundant protein (indicated by a circle) confirmed that of 126 detected peptides, up to 40 matched with the theoretical tryptic peptides of the *sidD* encoded NRP synthetase, providing sequence coverage of HMMP1/SidD up to 22.8% (m/z -tolerance: 1.5 Da) (Fig. 4C). Several peptides, which corresponded to theoretical tryptic fragments of the SidD, were sequenced by MALDI LIFT-ToF/ToF mass spectrometry [25] (Fig. 4C; Table 2). Post-source decay (PSD) fragmentation of the peptide with a mono-isotopic mass of 1498.744 Da revealed the amino acid sequence VELGEIESQLRAR and matched 100% with the theoretical sequence of a SidD peptide of 1498.810 Da (Fig. 4C). All resultant amino acid sequences correlated with the corresponding theoretical peptides of SidD, thereby confirming HMMP1 as the *sidD*-encoded NRP synthetase, which is very likely to be involved in siderophore biosynthesis in *A. fumigatus*.

At 48 h and absence of iron, another HMMP is apparent at a molecular mass of 300–400 kDa (HMMP2). Due to its size and apparent iron responsiveness, HMMP2 was proposed to correlate to another NRPS, which may be involved in siderophore biosynthesis in *A. fumigatus* and encoded by *sidC*. Attempts to separate and concentrate HMMP2 by means of gel permeation or ion exchange chromatography were unsuccessful (data not shown), probably due to its susceptibility to degradation. However, peptide mass fingerprinting of HMMP2, obtained following electrophoretic separation (Fig. 4A), yielded 88 peptides as detected by MALDI-ToF analysis, of which 68 matched with predicted tryptic peptides of the SidC (Fig. 4D). Thus, a sequence coverage of 18.6% (m/z -tolerance: 1.5 Da) for HMMP2/SidC was determined which, when combined with the appearance of this protein under conditions of iron depletion, strongly indicates that HMMP2 was at least a component of the *sidC*-encoded NRPS (theoretical mass: 496 kDa). The presence of SidE could not be detected by MALDI-ToF analysis. However, La Clair et al. [34] recently proposed the use

of biotin or fluorescently labeled coenzyme A analogs, in association with functional 4'-phosphopantetheinyl transferase activity, to label native NRPS and thereby facilitate purification [34]. Such an approach may prove useful for the purification of additional, low abundance, peptide synthetases (e.g., SidE) in *A. fumigatus*.

In summary, the iron-mediated, differential expression of two NRPS has been demonstrated in *A. fumigatus*. Furthermore, two proteins, namely SidD and C, involved in siderophore biosynthesis have been purified, analyzed by SDS-PAGE/2D-PAGE and identified by MALDI-ToF/MALDI LIFT-ToF/ToF mass spectrometry. This work furthers our understanding of siderophore biosynthesis in this organism and offers new insights in iron regulation of gene expression in *Aspergillus* spp.

Acknowledgments

This work was financially supported by the Higher Education Authority of Ireland under the Programme for Research in Third Level Institutions (HEA-PRTL). Claire Neville was a recipient of a Daniel O'Connell Fellowship from NUI Maynooth. Preliminary sequence data were obtained from The Institute for Genomic Research website at <http://www.tigr.org>. Sequencing of *Aspergillus fumigatus* was funded by the National Institute of Allergy and Infectious Disease U01 AI 48830 to David Denning and William Nierman, the Wellcome Trust, and Fondo de Investigaciones Sanitarias.

References

- [1] Kontoyiannis, D.P. and Bodey, G.P. (2002) Invasive aspergillosis in 2002: an update. *Eur. J. Clin. Microbiol. Infect. Dis.* 21, 161–172.
- [2] Mabey, J.E., Anderson, M.J., Giles, P.F., Miller, C.J., Attwood, T.K., Paton, N.W., Bornberg-Bauer, E., Robson, G.D., Oliver, S.G. and Denning, D.W. (2004) CADRE: the Central *Aspergillus* Data REpository. *Nucleic Acids Res.* 32, 401–405.
- [3] Schrettl, M., Bignell, E., Kragl, C., Joechl, C., Rogers, T., Arst Jr., H.N., Haynes, K. and Haas, H. (2004) Siderophore biosynthesis but not reductive iron assimilation is essential for *Aspergillus fumigatus* virulence. *J. Exp. Med.* 200, 1213–1219.

- [4] Liebmann, B., Muller, M., Braun, A. and Brakhage, A.A. (2004) The cyclic AMP-dependent protein kinase a network regulates development and virulence in *Aspergillus fumigatus*. *Infect. Immun.* 72, 5193–5203.
- [5] Bhabhra, R., Miley, M.D., Mylonakis, E., Boettner, D., Fortwendel, J., Panepinto, J.C., Postow, M., Rhodes, J.C. and Askew, D.S. (2004) Disruption of the *Aspergillus fumigatus* gene encoding nucleolar protein CgrA impairs thermotolerant growth and reduces virulence. *Infect. Immun.* 72, 4731–4740.
- [6] Hissen, A.H.T., Chow, J.M.T., Pinto, L.J. and Moore, M.M. (2004) Survival of *Aspergillus fumigatus* in serum involves removal of iron from transferrin: the role of siderophores. *Infect. Immun.* 72, 1402–1408.
- [7] Howard, D.H. (1999) Acquisition, transport, and storage of iron by pathogenic fungi. *Clin. Microbiol. Rev.* 12, 394–404.
- [8] Plattner, H.J. and Diekmann, H. (1994) Enzymology of siderophore biosynthesis in fungi In: *Metal Ions in Fungi* (Winkelmann, G. and Winge, D.R., Eds.), pp. 99–117. Decker, New York.
- [9] Eisendle, M., Oberegger, H., Zadra, I. and Haas, H. (2003) The siderophore system is essential for viability of *Aspergillus nidulans*: functional analysis of two genes encoding 1-ornithine N 5-monooxygenase (sidA) and a non-ribosomal peptide synthetase (sidC). *Mol. Microbiol.* 49, 359–375.
- [10] Lipmann, F. (1973) Non-ribosomal polypeptide synthesis. *Acta Endocrinol. Suppl. (Copenh)* 180, 294–300.
- [11] Kleinkauf, H. and von Döhren, H. (1990) Nonribosomal biosynthesis of peptide antibiotics. *Eur. J. Biochem.* 192, 1–15.
- [12] Keating, T.A. and Walsh, C.T. (1999) Initiation, elongation and termination strategies in polyketide and polypeptide antibiotic biosynthesis. *Curr. Opin. Chem. Biol.* 3, 598–606.
- [13] Cane, D.E. (1997) A special thematic issue on polyketide and nonribosomal polypeptide biosynthesis. *Chem. Rev.* 97, 2463–2706.
- [14] Haas, H. (2003) Molecular genetics of fungal siderophore biosynthesis and uptake: the role of siderophores in iron uptake and storage. *Appl. Microbiol. Biotechnol.* 62, 316–330.
- [15] Mei, B., Budde, A.D. and Leong, S.A. (1993) sid1, a gene initiating siderophore biosynthesis in *Ustilago maydis*: molecular characterisation, regulation by iron, and role in phytopathogenicity. *Proc. Natl. Acad. Sci. USA* 90, 903–907.
- [16] Yuan, W.M., Gentil, G.D., Budde, A.D. and Leong, S.A. (2001) Characterization of the *Ustilago maydis* sid2 gene, encoding a multidomain peptide synthetase in the ferrichrome biosynthetic gene cluster. *J. Bacteriol.* 183, 4040–4051.
- [17] Neville, C.M., Murphy, A., Kavanagh, K. and Doyle, S. (2005) A 4'-phosphopantetheinyl transferase mediates non-ribosomal peptide synthetase activation in *Aspergillus fumigatus*. *ChemBioChem* 6, 679–685.
- [18] Schwyn, B. and Neilands, J.B. (1987) Universal chemical assay for the detection and determination of siderophores. *Anal. Biochem.* 160, 47–56.
- [19] Milagres, A.M., Machuca, A. and Napoleaco, D. (1999) Detection of siderophore production from several fungi and bacteria by a modification of chrome azurol S (CAS) agar plate assay. *J. Microbiol. Meth.* 37, 1–6.
- [20] Burns, C., Geraghty, R., Neville, C., Murphy, A., Kavanagh, K. and Doyle, S. (2005) Identification, cloning and functional expression of three glutathione transferase genes from *Aspergillus fumigatus*. *Fungal Genet. Biol.* 42, 319–327.
- [21] Romero, B., Turner, G., Olivas, I., Laborda, F. and De Lucas, J.R. (2003) The *Aspergillus nidulans* alcA promoter drives tightly regulated conditional gene expression in *Aspergillus fumigatus* permitting validation of essential genes in this human pathogen. *Fungal Genet. Biol.* 40, 103–114.
- [22] Machesky, L.M., Reeves, E., Wientjes, F., Mattheyse, F.J., Grogan, A., Totty, N.F., Burlingame, A.L., Hsuan, J.J. and Segal, A.W. (1997) Mammalian actin-related protein 2/3 complex localizes to regions of lamellipodial protrusion and is composed of evolutionarily conserved proteins. *Biochem. J.* 15, 105–112.
- [23] Bradford, M.M. (1976) A rapid and sensitive method for the quantitation of microgram quantities of protein utilizing the principle of protein-dye binding. *Anal. Biochem.* 72, 248–254.
- [24] Laemmli, U.K. (1970) Cleavage of structural proteins during the assembly of the head of bacteriophage T4. *Nature* 227, 680–685.
- [25] Suckau, D., Resemann, A., Schuerenberg, M., Hufnagel, P., Franzen, J. and Holle, A. (2003) A novel MALDI LIFT-ToF/ToF mass spectrometer for proteomics. *Anal. Bioanal. Chem.* 376, 952–965.
- [26] von Döhren, H., Dickmann, R. and Pavela-Vrancic, M. (1999) The nonribosomal code. *Chem. Biol.* 6, 273–279.
- [27] Stachelhaus, T., Mootz, H.D. and Marahiel, M.A. (1999) The specificity-conferring code of adenylation domains in nonribosomal peptide synthetases. *Chem. Biol.* 6, 493–505.
- [28] Challis, G.L., Ravel, J. and Townsend, C.A. (2000) Predictive, structure-based model of amino acid recognition by nonribosomal peptide synthetase adenylation domains. *Chem. Biol.* 7, 211–224.
- [29] Gokhale, R.S. and Khosla, C. (2000) Role of linkers in communication between protein modules. *Curr. Opin. Chem. Biol.* 4, 22–27.
- [30] Reiber, K., Neuhoof, T., Ozegowski, J.H., von Döhren, H. and Schwecke, T. (2003) A nonribosomal peptide synthetase involved in the biosynthesis of ampullosporins in *Sepedonium ampullosporum*. *J. Pept. Sci.* 9, 701–713.
- [31] Correia, T., Grammel, N., Ortel, I., Keller, U. and Tudzynski, P. (2003) Molecular cloning and analysis of the ergopeptide assembly system in the ergot fungus *Claviceps purpurea*. *Chem. Biol.* 10, 1281–1292.
- [32] Nilius, A.M. and Farmer, S.G. (1990) Identification of extracellular siderophores of pathogenic strains of *Aspergillus fumigatus*. *J. Med. Vet. Mycol.* 28, 395–403.
- [33] Oberegger, H., Schoeser, M., Zadra, I., Abt, B. and Haas, H. (2001) SREA is involved in regulation of siderophore biosynthesis, utilization and uptake in *Aspergillus nidulans*. *Mol. Microbiol.* 41, 1077–1089.
- [34] La Clair, J.J., Foley, T.L., Schegg, T.R., Regan, C.M. and Burkart, M.D. (2004) Manipulation of carrier proteins in antibiotic biosynthesis. *Chem. Biol.* 11, 195–201.